

# Multipoint Anchoring of the [2.2.2]Metacyclophane Motif to a Gold Surface via Self-Assembly: Coordination Chemistry of a Cyclic Tetrakisocyanide Revisited

Masaharu Toriyama,<sup>†</sup> Tiffany R. Maher,<sup>‡</sup> Thomas C. Holovics,<sup>‡</sup> Kumar Vanka,<sup>‡</sup> Victor W. Day,<sup>‡</sup> Cindy L. Berrie,<sup>‡</sup> Ward H. Thompson,<sup>‡</sup> and Mikhail V. Barybin<sup>\*‡</sup>

Department of Chemistry, The University of Kansas, Lawrence, Kansas 66045, and College of Pharmacy, Nihon University, 7-7-1 Narashinodai, Funabashi-shi, Chiba 274-8555, Japan

Received December 12, 2007

A one-pot transformation of bis(2-isocyano-3-methylphenyl)ethane affords gram quantities of 8,16,24,32-tetrakisocyanato[2.2.2]metacyclophane (**3**). The solid state structure of **3** is remarkably close to the lowest energy conformation found on the potential energy landscape for **3** by DFT. In solution, the structure of metacyclophane **3** is mobile but can be locked in a rectangular *gauche*–*anti*–*gauche*–*anti* conformation by coordination of the isocyanide substituents to the  $[W(CO)_5]$  units to give  $[M]_4(\mu_4-\eta^1:\eta^1:\eta^1:\eta^1-\mathbf{3})$  (**5**). The tetranuclear  $[M]_4(\mu_4-\eta^1:\eta^1:\eta^1:\eta^1-\mathbf{3})$  motif featured in crystallographically characterized **5** may be present in several insoluble complexes of **3** previously described as mononuclear  $\eta^4$  species. A self-assembled monolayer of metacyclophane **3** is formed upon exposing a solution of **3** to the gold(111) surface with no precautions to exclude air or light. The monolayer nature of the film was confirmed by optical ellipsometry. The isocyanide stretching band for **3** shifts from 2119  $\text{cm}^{-1}$  in solution to 2175  $\text{cm}^{-1}$  upon chemisorption to metallic gold. The FTIR spectrum of the film indicates interaction of **3** with the gold surface via all four of its isocyanide anchors. No gold-facilitated oxidation of the –NC junctions was detected under ambient conditions. The energy cost associated with accessing the conformations of **3** suitable for  $\mu_4-\eta^1:\eta^1:\eta^1:\eta^1$  interaction of the molecule with the Au(111) surface is under 8 kcal/mol, a value that can be easily offset by formation of a gold–isocyanide bond. Two different  $\mu_4-\eta^1:\eta^1:\eta^1:\eta^1$  coordination arrangements of **3** with respect to gold atoms on the (111) face of the fcc Au lattice are suggested.

## Introduction

Coordination chemistry of polyisocyanide ligands has been attracting substantial multidisciplinary interest,<sup>1</sup> more recently, with applications in materials science in mind.<sup>2–14</sup> Organic diisocyanides, both naturally occurring<sup>15</sup> and syn-

thetic,<sup>16</sup> constitute the most common class of polyisocyanides and have been explored in the design of molecular wires, switches, memory cells, functionalized organic surfaces, solar energy storage devices, etc.<sup>3–14,17</sup> Bidentate isocyanide ligands can either bridge two metal atoms within a dinuclear

\* To whom correspondence should be addressed. E-mail: mbarybin@ku.edu.

<sup>†</sup> On sabbatical leave from Nihon University.

<sup>‡</sup> The University of Kansas.

- (1) Hahn, F. E. *Angew. Chem., Int. Ed. Engl.* **1993**, *32*, 650–665.
- (2) Harvey, P. D. *J. Inorg. Organomet. Polym.* **2004**, *14*, 211–226.
- (3) Siemeling, U.; Rother, D.; Bruhn, C.; Fink, H.; Weidner, T.; Traeger, F.; Rothenberger, A.; Fenske, D.; Priebe, A.; Maurer, J.; Winter, R. *J. Am. Chem. Soc.* **2005**, *127*, 1102–1103.
- (4) (a) DuBose, D. L.; Robinson, R. E.; Holovics, T. C.; Moody, D. R.; Weintrob, E. C.; Berrie, C. L.; Barybin, M. V. *Langmuir* **2006**, *22*, 4599–4606. (b) Holovics, T. C.; Robinson, R. E.; Weintrob, E. C.; Toriyama, M.; Lushington, G. H.; Barybin, M. V. *J. Am. Chem. Soc.* **2006**, *128*, 2300–2309.
- (5) Hong, S.; Reifenberger, R.; Tian, W.; Datta, S.; Henderson, J.; Kubiak, C. P. *Superlattices Microstruct.* **2000**, *28*, 289–303.

- (6) Chen, J.; Wang, W.; Klemic, J.; Reed, M. A.; Axelrod, B. W.; Kaschak, D. M.; Rawlett, A. M.; Price, D. W.; Dirk, S. M.; Tour, J. M.; Grubisha, D. S.; Bennett, D. W. *Ann. N.Y. Acad. Sci.* **2002**, *960* (Molecular Electronics II), 69–99.
- (7) Dahlke, R.; Schollwock, U. *Phys. Rev. B* **2004**, *69*, 085324.
- (8) Chen, J.; Calvet, L. C.; Reed, M. A.; Carr, D. W.; Grubisha, D. S.; Bennett, D. W. *Chem. Phys. Lett.* **1999**, *313*, 741–748.
- (9) Seminario, J. M.; Zacarias, A. G.; Tour, J. M. *J. Am. Chem. Soc.* **1999**, *121*, 411–416.
- (10) Stapleton, J. J.; Daniel, T. A.; Uppili, S.; Cabarcos, O. M.; Naciri, J.; Shashidhar, R.; Allara, D. L. *Langmuir* **2005**, *21*, 11061–11070.
- (11) Swanson, S. A.; McClain, R.; Lovejoy, K. S.; Alamdari, N. B.; Hamilton, J. S.; Scott, J. C. *Langmuir* **2005**, *21*, 5034–5039.
- (12) Murphy, K. L.; Tysoc, W. T.; Bennett, D. W. *Langmuir* **2004**, *20*, 1732–1738.
- (13) Pranger, L.; Goldstein, A.; Tannenbaum, R. *Langmuir* **2005**, *21*, 5396–5404.

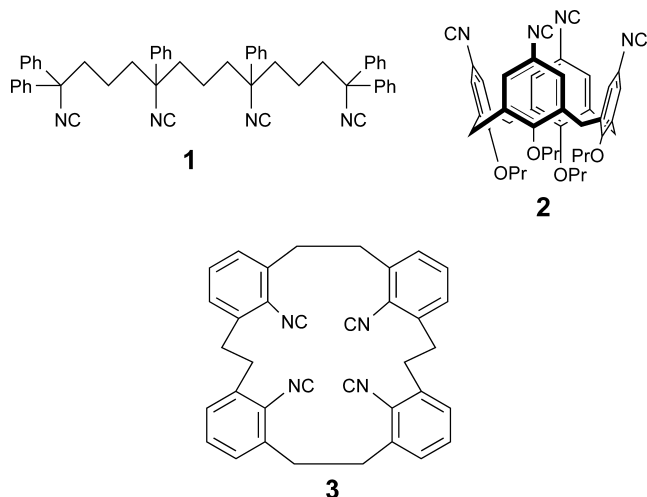


**Figure 1.** Organic tetraisocyanides involving linear (1),<sup>19</sup> calix[4]arene (2),<sup>20</sup> and [2.2.2.2]metacyclophane<sup>21</sup> (3) frameworks.

motif ( $\eta^1:\eta^1$  coordination) or form a mononuclear  $\eta^2$  chelate complex.<sup>1</sup> A few tridentate isocyanides that are currently known have linear,<sup>1</sup> trigonal,<sup>18</sup> or tripodal topology.<sup>1</sup> The tripodal triisocyanides can engage in both  $\eta^1:\eta^1:\eta^1$  (e.g., within a polymetallic cluster<sup>10</sup>) and  $\eta^3$  bonding with transition metals.<sup>1</sup>

To the best of our knowledge, only three organic tetraisocyanides have been reported to date, and their chemistry remains extremely scarce. The linear tetraisocyanide (1) described by Mann et al.<sup>19</sup> and shown in Figure 1 was used to assemble chains of Rh(I) ions by linking  $[\text{Rh}_2]^{2+}$  motifs, which, at the time, were explored for implementation in potential solar energy storage devices.<sup>17</sup> The recent tetraisocyanide functionalization of the upper rim of a calix[4]arene (compound 2, Figure 1) by Harvey<sup>20</sup> and co-workers afforded an attractive 3D-building block for new polymetallic coordination architectures. In 1986, Ito et al.<sup>21</sup> reported synthesis of the tetraisocyanide-substituted [2.2.2.2]metacyclophane (3) shown in Figure 1 and concluded that this tetraisocyanide functions as a chelating  $\eta^4$ -ligand to Cu(I), Co(II), and Ni(0) (e.g., Figure 2a). However, the ability of this ligand to coordinate to a single metal center via all four of its isocyanide groups was doubted by Hahn in his 1993 review.<sup>1</sup> No further reports involving tetraisocyanide 3 have appeared since then.

The three complexes of 3 described by Ito and co-workers are insoluble in common solvents, and their characterization was limited to solid-state IR and elemental analysis.<sup>21</sup> We

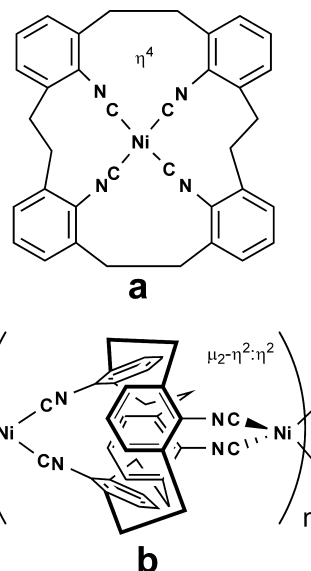


**Figure 2.** (a) Previously proposed<sup>21</sup> structure of the Ni<sup>0</sup> adduct of 3 and (b) one of the possible alternative oligomeric descriptions of this complex.

note that neither of these methods excludes the possibility of forming oligomeric ensembles, an example of which is illustrated in Figure 2b for the Ni(0) adduct of 3 (cf. coordination polymers based on tetrafunctionalized calix[4]arenes<sup>2</sup>). In fact, the lack of solubility of these species is highly suggestive of their polymeric nature. In addition, the  $\eta^4$  coordination of 3 would require, at the very least, severe bending of the C–N–C units, which is not reflected in the  $\nu_{\text{CN}}$  data<sup>21</sup> documented for either of its complexes.

Given the important role of cyclophanes in molecular recognition research<sup>22</sup> and recent progress in the surface chemistry of isocyanoarenes,<sup>3–14</sup> we became interested in the coordination chemistry of polyisocyanide-substituted cyclophanes with the goal of employing isocyanide groups as two-atom long “anchors” to self-assemble cyclophane-based organic surfaces. Even though self-assembled monolayers (SAMs) of benzenoid isocyanoarenes on Au(111) are prone to rapid deterioration upon exposure to ambient atmosphere due to gold-facilitated oxidation<sup>23</sup> of the isocyanide junctions to isocyanate,<sup>10</sup> SAMs of polyisocyanocyclophanes on Au(111) may be expected to exhibit enhanced kinetic stability because they would feature several coordinated isocyanoarene moieties linked together. Herein, we revisit the synthesis and structure of tetraisocyanide [2.2.2.2]metacyclophane 3 and describe its  $\eta^1:\eta^1:\eta^1:\eta^1$  coordination to discrete monotopic transition metal units, as well as to a metallic gold surface.

## Experimental Section

**General Procedures and Starting Materials.** Unless specified otherwise, synthetic operations were performed under an atmosphere

- (14) Ansell, M. A.; Cogan, E. B.; Page, C. J. *Langmuir* **2000**, *16*, 1172–1179.  
 (15) (a) Garson, M. J.; Simpson, J. S. *Nat. Prod. Rep.* **2004**, *21*, 164–179.  
 (b) Chang, C. W. J. *Prog. Chem. Org. Nat. Prod.* **2000**, *80*, 1–186.  
 (c) Chang, C. W. J.; Scheuer, P. J. *Top. Curr. Chem.* **1993**, *167*, 33–75.  
 (16) Ugi, I. *Isonitrile Chemistry*; Academic Press: New York, 1971.  
 (17) Gray, H. B.; Maverick, A. W. *Science* **1981**, *214*, 1201–1205.  
 (18) Paek, J. H.; Song, K. H.; Jung, I.; Kang, S. O.; Ko, J. *Inorg. Chem.* **2007**, *46*, 2787–2796.  
 (19) Hill, M. G.; Comstock, M. C.; Mann, K. R. *J. Org. Chem.* **1990**, *55*, 4950–4951.  
 (20) Gagnon, J.; Drouin, M.; Harvey, P. D. *Inorg. Chem.* **2001**, *40*, 6052–6056.  
 (21) Ito, Y.; Kobayashi, K.; Saegusa, T. *J. Organomet. Chem.* **1986**, *303*, 301–308.

- (22) (a) Tobe, Y.; Sonoda, M. In *Modern Cyclophane Chemistry*; Gleiter, R., Hopf, H., Eds.; Wiley-VCH: Weinheim, Germany, 2004. (b) Diederich, F. In *Cyclophanes*, Stoddart, J. F., Ed.; Monographs in Supramolecular Chemistry; The Royal Society of Chemistry: Cambridge, U.K., 1991.  
 (23) McDonagh, A. M.; Zareie, M. H.; Ford, M. J.; Barton, C. S.; Ginic-Markovic, M.; Matison, J. G. *J. Am. Chem. Soc.* **2007**, *129*, 3533–3538.

of 99.5% argon purified by passage through columns of activated BASF catalyst and molecular sieves. Solutions were transferred via stainless steel needles whenever possible. Standard Schlenk techniques were employed with a double manifold vacuum line. Solvents, including deuterated solvents, were freed of impurities by standard procedures<sup>24</sup> and stored under argon.

Infrared spectra were recorded on Shimadzu FTIR-8400S or JASCO FT/IR-300E spectrometers. NMR samples were analyzed on Bruker Avance 400 or 500 spectrometers. <sup>1</sup>H and <sup>13</sup>C NMR chemical shifts are given with reference to residual <sup>1</sup>H solvent resonances relative to SiMe<sub>4</sub>. Melting points are uncorrected and were determined for samples in sealed capillary tubes. High-resolution mass spectra (HR-MS) were recorded on a JEOL GCmate instrument. Elemental analyses were carried out by Desert Analytics, Tucson, Arizona. 1,2-Bis(2-isocyano-3-methylphenyl)ethane was prepared from commercial 2,6-xylyl isocyanide (Fluka) according to a literature procedure.<sup>21</sup> All other reagents were obtained from commercial sources and freed of oxygen and moisture if used in air- or water-sensitive syntheses. Davisil (200–425 mesh, type 60A) silica gel was used for chromatographic purifications.

**Synthesis of 8,16,24,32-Tetraisocyano[2.2.2.2]metacyclophane (3).** This synthesis is a modified, scaled-up version of that reported by Ito et al.<sup>21</sup> A solution of <sup>n</sup>BuLi in hexane (1.57 mol/L, 61.2 mL, 96 mmol) was slowly transferred to a solution of diisopropylamine (13.9 mL, 98 mmol) in 720 mL of diglyme at –78 °C. The mixture was stirred for 1 h. Then, a solution of 1,2-bis(2-isocyano-3-methylphenyl)ethane (6.25 g, 24 mmol) in 180 mL of diglyme was added over a period of 30 min, and the resulting mixture was stirred at –78 °C for 1 h. 1,2-Dibromoethane (18.22 g, 98 mmol) was added dropwise, and the reaction mixture continued to be stirred at –78 °C for 12 h. The reaction was then quenched in air by addition of saturated aqueous NH<sub>4</sub>Cl (50 mL) and warmed to 20 °C. The mixture was poured into aqueous NH<sub>4</sub>Cl/CHCl<sub>3</sub>. The resulting slurry was filtered, and the chloroform layer was washed with water and then brine, dried over anhydrous Na<sub>2</sub>SO<sub>4</sub>, and evaporated to dryness *in vacuo*. The residue was subjected to column chromatography (silica gel, neat CH<sub>2</sub>Cl<sub>2</sub>), which afforded colorless crystalline **3** (1.74 g, 3.37 mmol) in a 28% yield after recrystallization of the crude product from C<sub>6</sub>H<sub>6</sub>/MeOH. HR-MS (EI+, *m/z*): calcd for C<sub>36</sub>H<sub>28</sub>N<sub>4</sub> (M<sup>+</sup>) 516.23948; found 516.23146. IR (KBr):  $\nu_{\text{CN}}$  2116 vs cm<sup>-1</sup>. <sup>1</sup>H NMR (500 MHz, CDCl<sub>3</sub>, 25 °C):  $\delta$  3.05 (s, 4H), 6.94 (d, 2H, <sup>3</sup>J<sub>HH</sub> = 8 Hz), 7.17 (t, 1H, <sup>3</sup>J<sub>HH</sub> = 8 Hz). <sup>13</sup>C{<sup>1</sup>H} NMR (125.65 MHz, CDCl<sub>3</sub>, 25 °C):  $\delta$  31.1 (CH<sub>2</sub>), 126.6, 127.5, 129.3, 136.7 (aromatic C), 168.9 (CNR) ppm.

The above chromatographic procedure also allowed isolation of the hexameric cyclic congener of **3**, namely, hexaisocyano[2.2.2.2.2.2]metacyclophane (**4**) (0.19 g, 0.25 mmol), in a 3% yield. HR-MS (EI+, *m/z*): calcd for C<sub>54</sub>H<sub>42</sub>N<sub>6</sub> (M<sup>+</sup>) 774.35517; found 774.34789. IR (KBr):  $\nu_{\text{CN}}$  2116 vs cm<sup>-1</sup>. <sup>1</sup>H NMR (500 MHz, CDCl<sub>3</sub>, 25 °C):  $\delta$  3.04 (s, 4H), 6.93 (d, 2H, <sup>3</sup>J<sub>HH</sub> = 8 Hz), 7.11 (t, 1H, <sup>3</sup>J<sub>HH</sub> = 8 Hz). <sup>13</sup>C{<sup>1</sup>H} NMR (125.65 MHz, CDCl<sub>3</sub>, 25 °C):  $\delta$  32.6 (CH<sub>2</sub>), 126.3, 128.3, 129.1, 137.5 (aromatic C), 169.2 (CNR) ppm.

**Synthesis of [(OC)<sub>5</sub>W]<sub>4</sub>( $\mu_4$ - $\eta^1$ : $\eta^1$ : $\eta^1$ : $\eta^1$ -8,16,24,32-Tetraisocyano[2.2.2.2]metacyclophane (5).** W(CO)<sub>5</sub>(THF) was generated *in situ* by photolysis of W(CO)<sub>6</sub> (0.510 g, 1.45 mmol) dissolved in 80 mL of THF using a Hanovia Hg 450 W immersion lamp. After the formation of W(CO)<sub>5</sub>(THF) had been judged nearly complete by FTIR in the  $\nu_{\text{CO}}$  region (ca. 4 h), the resulting orange solution was transferred to a solution of **3** (0.150 g, 0.290 mmol)

in 20 mL of THF dropwise via cannula at rt. The mixture was stirred for 15 h while it turned a pale yellow color. Then, the content of the reactor was open to air, and all solvent was removed under vacuum. The residue was passed through a short silica gel column using neat CH<sub>2</sub>Cl<sub>2</sub>. After solvent removal and drying at 10<sup>-2</sup> Torr, tan crystalline **5** (0.520 g, 0.287 mmol) was isolated in a 99% yield based on the tetraisocyanide used. Mp 215–218 °C (dec). Anal. Calcd for C<sub>56</sub>H<sub>28</sub>N<sub>4</sub>O<sub>20</sub>W<sub>4</sub>: C, 37.12; H, 1.56; N, 3.09. Found: C, 36.92; H 1.46; N, 3.03. IR (CH<sub>2</sub>Cl<sub>2</sub>):  $\nu_{\text{CN}}$  2133 w,  $\nu_{\text{CO}}$  2052 m, 1954 s, 1940 vs cm<sup>-1</sup>. <sup>1</sup>H NMR (500 MHz, CD<sub>2</sub>Cl<sub>2</sub>, 25 °C):  $\delta$  2.75 (br s, 2H), 3.09 (br s, 2H), 7.38 (d, 2H, <sup>3</sup>J<sub>HH</sub> = 8 Hz), 7.51 (t, 1H, <sup>3</sup>J<sub>HH</sub> = 8 Hz) ppm.

**X-ray Structure Determination for 3 and 5·2CH<sub>2</sub>Cl<sub>2</sub>.** X-ray quality crystals of both **3** and **5**·2CH<sub>2</sub>Cl<sub>2</sub> were grown by layering pentane over nearly saturated solutions of these compounds in CH<sub>2</sub>Cl<sub>2</sub> at 22 °C and then cooling the samples to +4 °C for several days. All manipulations with the crystals prior to transfer to the goniometer were performed in air. Intensity data for both samples were collected using a Bruker APEX CCD area detector mounted on a Bruker D8 goniometer employing graphite-monochromated Mo K $\alpha$  radiation ( $\lambda$  = 0.71073 Å). The space groups were determined by systematic absences or statistical tests and verified by subsequent refinements. All structures were solved by direct methods and refined by full-matrix least-squares methods on *F*<sup>2</sup>. Non-hydrogen atoms were refined anisotropically. Hydrogen atom positions were initially determined by geometry and refined by a riding model. Hydrogen atom displacement parameters were set to 1.2 times the displacement parameters of the bonded atoms. All calculations employed the SHELXTL V5.0 suite of programs (SHELXTL-Plus V5.0, Siemens Industrial Automation, Inc., Madison, WI). In both cases, the data were corrected for absorption by the empirical method.<sup>25</sup> For **5**·2CH<sub>2</sub>Cl<sub>2</sub>, the top 20 residual peaks, as well as the minimum hole of –1.83 e/Å<sup>3</sup>, in the final difference map were within 1.16 Å of a tungsten atom. Crystal data, data collection, solution, and refinement information for **3** and **5**·2CH<sub>2</sub>Cl<sub>2</sub> are summarized in Table 1. Details of the X-ray work can be found in the Supporting Information.

**Surface Studies. (a) Monolayers of 3 on the Au(111) Surface.** Gold-coated mica substrates with 1500 Å of Au(111) covering 2.0 cm × 1.6 cm were purchased from Molecular Imaging Corp. These commercial substrates were soaked in dichloromethane, acetone, and methanol for 2 h in each solvent, then rinsed thoroughly with hot methanol and dried under a stream of nitrogen immediately before use. Monolayer films were formed by immersing the freshly cleaned metal substrate (gold on mica) into a ca. 2 mM solution of **3** in CH<sub>2</sub>Cl<sub>2</sub>. No precautions to exclude air or ambient laboratory lighting were taken. After ca. 24 h, the gold samples were removed, rinsed thoroughly with CH<sub>2</sub>Cl<sub>2</sub>, and dried under a flow of nitrogen gas.

**(b) Optical Ellipsometry.** The film thicknesses were determined using an Auto EL III ellipsometer (Rudolph Research). All measurements were made with a HeNe laser at a wavelength of 632.4 nm and an incident angle of 70°. The optical constants for the gold films were determined for each sample individually from the measurements on the freshly cleaned bare gold sample. The average optical constants for the samples analyzed in these experiments were *n* = 0.155 and *k* = 3.503. These optical constants provided input for the substrate properties in the determination of the thickness of the adsorbed organic layer. A refractive index of

(24) Gordon, A. J.; Ford, R. A. *The Chemist's Companion: A Handbook of Practical Data, Techniques, and References*, 1st ed.; Wiley & Sons: New York, 1973.

(25) Sheldrick, G. M. *SADABS. Program for Empirical Absorption Correction of Area Detector Data*; University of Göttingen: Göttingen, Germany, 2000.



**Table 1.** Crystal Data, Data Collection and Refinement Information for **3** and **5**·2CH<sub>2</sub>Cl<sub>2</sub>

	<b>3</b>	<b>5</b> ·2CH <sub>2</sub> Cl <sub>2</sub>
empirical formula	C <sub>36</sub> H <sub>28</sub> N <sub>4</sub>	C <sub>58</sub> H <sub>32</sub> Cl <sub>4</sub> N <sub>4</sub> O <sub>20</sub> W <sub>4</sub>
fw	516.62	1982.08
temp (K)	100(2)	100(2)
cryst syst	monoclinic	triclinic
space group	P2 <sub>1</sub> /c	P $\bar{1}$
a (Å)	12.8787(5)	9.6788(6)
b (Å)	14.0977(6)	12.8891(8)
c (Å)	16.1673(6)	25.7314(15)
α (deg)	90	84.727(1)
β (deg)	106.795(2)	89.430(1)
γ (deg)	90	76.445(1)
V (Å <sup>3</sup> )	2810.1(2)	3107.2(3)
Z	4	2
D <sub>calcd</sub> (Mg m <sup>-3</sup> )	1.221	2.119
abs coeff (mm <sup>-1</sup> )	0.073	7.629
F(000)	1088	1864
cryst size (mm <sup>3</sup> )	0.54 × 0.45 × 0.18	0.14 × 0.09 × 0.08
θ range for data collection (deg)	1.95–30.53	2.31–30.04
reflns collected	23528	37009
reflns unique	8442	17921
R <sub>int</sub> <sup>a</sup>	0.024	0.081
abs corr	SADABS	SADABS
max and min trans	0.987 and 0.962	0.763 and 0.486
refinement method	full-matrix least-squares on F <sup>2</sup>	
data/restraints/params	8442/0/361	17921/27/832
GOF on F <sup>2</sup>	1.032	0.933
final R indices [I > 2σ(I)] <sup>b</sup>	R <sub>1</sub> = 0.050	R <sub>1</sub> = 0.065
	wR <sub>2</sub> = 0.128	wR <sub>2</sub> = 0.113
R indices (all data) <sup>b</sup>	R <sub>1</sub> = 0.060	R <sub>1</sub> = 0.115
	wR <sub>2</sub> = 0.135	wR <sub>2</sub> = 0.128
largest diff peak and hole (e·Å <sup>-3</sup> )	0.42 and -0.23	3.02 and -1.83

<sup>a</sup> R<sub>int</sub> = Σ|F<sub>o</sub><sup>2</sup> - ⟨F<sub>o</sub><sup>2</sup>⟩|/Σ|F<sub>o</sub><sup>2</sup>|; <sup>b</sup> R<sub>1</sub> = Σ||F<sub>o</sub> - |F<sub>c</sub>||/Σ|F<sub>o</sub>|; wR<sub>2</sub> = [Σ(w(F<sub>o</sub><sup>2</sup> - F<sub>c</sub><sup>2</sup>)/Σ(w(F<sub>o</sub><sup>2</sup>)))]<sup>1/2</sup>.

1.45 was assumed<sup>26</sup> for the organic thin films reported herein. Measurements were taken at a minimum of four different spots on each sample. The reported thickness constitutes an average of the measurements over each of those spots along with the standard deviation of the measurement.

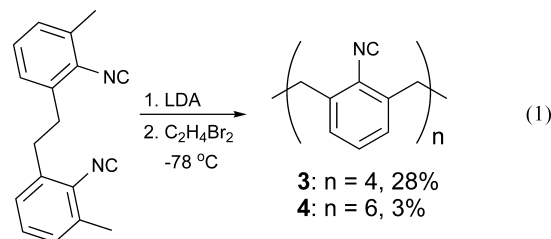
(c) **FTIR.** The grazing incidence reflection-absorption Fourier transform infrared spectroscopy data were collected on a nitrogen-purged Thermo Nicolet 670 FTIR spectrometer with a VeeMax grazing angle accessory set at an angle of 70°. A freshly cleaned bare gold substrate was used to collect a background spectrum before each experiment. Ten thousand scans from 600 to 4000 cm<sup>-1</sup> at 4 cm<sup>-1</sup> resolution were collected for each background/sample pair.

**DFT Calculations.** Density functional theory (DFT) electronic structure calculations on **3** were carried out with the Gaussian 03 program<sup>27</sup> using the B3LYP functional<sup>28</sup> with 3-21G\* and 6-31+G\* basis sets (*vide infra*). The potential energy landscape for **3** features

multiple local minima due to combinations of the various possible dihedral angles for the four C-CH<sub>2</sub>-CH<sub>2</sub>-C units within **3** (cf. potential energy as a function of the dihedral angle for butane<sup>29</sup>). The initial screening of the conformations of **3** that are suitable for binding to the Au(111) surface via all four isocyanide groups in the upright fashion was conducted using the 3-21G\* basis set for reasons of computational cost. The two lowest energy structures provided by this analysis, out of ten screened, were then optimized at the 6-31+G\* level.

## Results and Discussion

**Synthetic Work.** Despite the provocative report on the formation of several mononuclear complexes of tetraisocyanide **3** two decades ago<sup>21</sup> and the subsequent doubt regarding their η<sup>4</sup> nature,<sup>1</sup> the chemistry of **3** has remained unexplored. In part, this may be attributed to the fact that the preparation of reasonable quantities of [2.2.2.2]metacyclophanes, especially those possessing functional groups, is often tedious at best.<sup>30</sup> For example, the original isolation of crude **3** was performed on a rather small scale and involved a preparative TLC procedure.<sup>21</sup>



Our modified synthesis of **3** is conducted on a substantially larger scale and allows isolation of this functionalized metacyclophane in nearly 2 g quantities at a time. Addition of a solution of 1,2-bis(2-isocyano-3-methylphenyl)ethane to an *in situ* generated solution of lithium diisopropylamide (LDA) followed by treatment of the resulting dilithiated diisocyanide with 1,2-dibromoethane at -78 °C effected oxidative oligomerization of the starting diisocyanide species (eq 1). After aqueous workup, column chromatography of the reaction mixture on silica using neat CH<sub>2</sub>Cl<sub>2</sub> afforded colorless crystalline **3** in ca. 30% yield. The hitherto unknown hexaisocyanide analogue of **3** (compound **4**) was isolated from the reaction mixture as well, albeit in a much lower yield (eq 1). Notably, compound **4** constitutes an exceedingly rare example of a functionalized [2.2.2.2.2.2]metacyclophane with saturated linkers.<sup>31</sup> No attempts to resolve individual components from the remaining mixture of higher oligoisocyanide products were made. Unlike 2,6-xylyl isocyanide (CNXyl), which is the monomeric analogue and precursor of **3** and **4**, crystalline **3** and **4** can be stored in air at room temperature for at least a year without detectable deterioration. While homologues **3** and **4** have virtually identical FTIR

(26) (a) Clear, S. C.; Nealey, P. F. *Langmuir* **2001**, *17*, 720–732. (b) Le Grange, J. D.; Markham, J. L.; Kurkjian, C. R. *Langmuir* **1993**, *9*, 1749–1753. (c) Wasserman, S. R.; Whitesides, G. M.; Tidswell, I. M.; Ocko, B. M.; Pershan, P. S.; Axe, J. D. *J. Am. Chem. Soc.* **1989**, *111*, 5852–5861.

(27) Frisch, M. J., et al. *Gaussian 03*, Revision C.02; Gaussian, Inc.: Wallingford, CT, 2004.

(28) (a) Miehlich, B.; Savin, A.; Stoll, H.; Preuss, H. *Chem. Phys. Lett.* **1989**, *157*, 200–206. (b) Lee, C.; Yang, W.; Parr, R. G. *Phys. Rev. B* **1988**, *37*, 785–789.

(29) Allinger, N. L.; Fermann, J. T.; Allen, W. D.; Schaefer, H. F., III *J. Chem. Phys.* **1997**, *106*, 5143–5150.

(30) Tashiro, M.; Watanabe, T.; Tsuge, A.; Sawada, T.; Mataka, S. *J. Org. Chem.* **1989**, *54*, 2632–2638.

(31) For chemistry of the increasingly popular [2.2.2.2.2.2]metacyclophane-1,9,17,25,33,41-hexaynes featuring unsaturated -C≡C- linkers, see: Traber, B.; Oeser, T.; Gleiter, R. *Eur. J. Org. Chem.* **2005**, *7*, 1283–1292, and references therein.

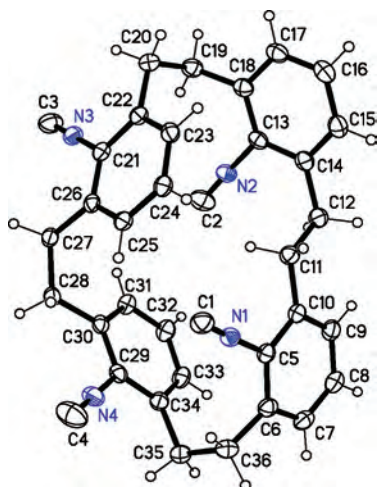
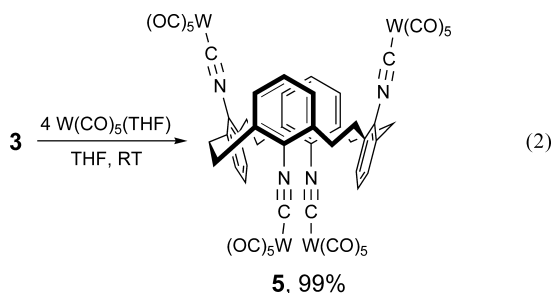


**Figure 3.** Molecular structure of **3** in the solid state (50% thermal ellipsoids).

and  $^1\text{H}$  and  $^{13}\text{C}$  NMR signatures, they can be easily distinguished by means of the mass-spectral analysis (Figures S1–S8). Both metacyclophanes are mobile<sup>30</sup> on the NMR time scale in solution at 25 °C as evidenced by a singlet  $-\text{CH}_2-$  resonance at ca. 3.0 ppm.

Treatment of **3** with a slight excess  $\text{W}(\text{CO})_5(\text{THF})$ , a synthon for the 16-electron “ $\text{W}(\text{CO})_5$ ” motif, quantitatively produced its tetrametallic adduct **5** (eq 2). Similar to free **3**, complex **5** is stable in the solid state for extended periods under ambient conditions. Upon interaction of **3** with  $\text{W}(\text{CO})_5(\text{THF})$ , the  $\nu_{\text{CN}}$  peak at  $2116\text{ cm}^{-1}$  corresponding to the free isocyanide groups in **3** was replaced by the new  $\nu_{\text{CN}}$  band at  $2133\text{ cm}^{-1}$  assignable to the  $\text{W}(\text{CO})_5(\text{CNAr}^{\text{yl}})$  moiety. Whereas all four  $[\text{W}(\text{CO})_5(\text{CNC}_6\text{H}_3)]$  fragments within tetramer **5** are mutually equivalent on the NMR time scale at 25 °C, the  $^1\text{H}$  NMR spectrum of this complex at 25 °C shows two distinct, albeit somewhat broad, resonances of equal intensities at 2.75 and 3.09 ppm that correspond to the  $-\text{CH}_2\text{CH}_2-$  units of **5** (Figure S9). No cross-peaks relating these two resonances are present in the corresponding 2D  $^1\text{H}$  COSY map (Figure S10). These observations are consistent with (a) **5** featuring two pairs of linker environments (*vide infra*) that are distinguishable on the NMR time scale at 25 °C and (b) all H-nuclei within an individual  $-\text{CH}_2-\text{CH}_2-$  unit being equivalent on the NMR time scale at 25 °C. The bulky nature of the  $[-\text{NCW}(\text{CO})_5]$  groups is, presumably, responsible for locking metacyclophane **5** in a specific conformation.



**Structural Characterization of 3 and 5.** In addition to HRMS, the tetrameric nature of **3** was confirmed by single-crystal X-ray crystallography (Figure 3). The four aryl

**Table 2.** Selected Bond Distances, Angles, and Torsional Angles for **3** and **5**·2CH<sub>2</sub>Cl<sub>2</sub>

<b>3</b> (DFT) <sup>a</sup>	<b>3</b> (X-ray)	<b>5</b> ·2CH <sub>2</sub> Cl <sub>2</sub> (X-ray)
	C–NC <sub>6</sub> [Å]	
1.179	1.157(2)	1.16(1)
1.179	1.157(2)	1.16(1)
1.178	1.156(2)	1.16(1)
1.178	1.156(2)	1.11(1)
	CN–C <sub>6</sub> [Å]	
1.391	1.407(2)	1.41(1)
1.390	1.407(2)	1.40(1)
1.390	1.405(2)	1.40(1)
1.390	1.403(2)	1.39(1)
	W–C [Å]	
		2.17(1)
		2.12(1)
		2.12(1)
		2.11(1)
	C–N–C [deg]	
179.3	179.6(2)	173(1)
179.1	178.1(2)	168(1)
177.7	177.4(2)	168(1)
176.7	177.4(2)	168(1)
	C–CH <sub>2</sub> –CH <sub>2</sub> –C [deg]	
165.6	173.3(1)	172(1)
66.0	69.0(1)	171(1)
62.7	58.4(1)	63(1)
54.9	48.4(1)	62(1)

<sup>a</sup> Lowest energy conformation found in this study.

isocyanide moieties within **3** are very similar to each other in terms of their metric characteristics (Table 2). The C–NC and CN–C<sub>6</sub> distances, as well as the C–N–C angles, observed for **3** are close to the corresponding values reported for CNXyl, the monomeric analogue of **3** (C–NXyl 1.160(3) Å, CN–Xyl 1.399(2) Å, C–N–C 179.4(2) Å<sup>32</sup>). The solid-state structure of **3** exhibits one *anti* and three *gauche* configurations of the C–CH<sub>2</sub>–CH<sub>2</sub>–C units<sup>33</sup> and is remarkably similar to the lowest energy conformation found in our DFT study of the molecule (Table 2, Figure 4). Thus, crystal packing forces play a relatively minor role in determining the geometry of **3** in the solid state. This is contrary to a previous report that suggested that packing effects have a significant influence on the conformation of the “parent” unsubstituted [2.2.2.2]metacyclophane, C<sub>32</sub>H<sub>32</sub>, the X-ray structure of which features alternating *anti* (177°) and *gauche* (68°) bridges.<sup>34</sup>

Upon  $\eta^1:\eta^1:\eta^1:\eta^1$  complexation of **3** with four  $[\text{W}(\text{CO})_5]$  units to give **5**, the rather irregularly shaped free tetra-isocyanide ligand (Figures 3 and 4) transforms into a substantially more symmetric motif. Indeed, the X-ray structure of **5** contains pairs of virtually identical alternating *gauche* and *anti* linkers that connect four  $[(\text{OC})_5\text{W}(\text{CNAr}^{\text{yl}})]$  fragments (Figure 5, Table 2). The  $-\text{NCW}(\text{CO})_5$  substituents alternate their “up” and “down” orientation with respect to the [2.2.2.2]metacyclophane ring, undoubtedly, to minimize repulsion between these bulky groups. The solid state conformation of **5** is fully consistent with the NMR characteristics of this

(32) Mathieson, T.; Schier, A.; Schmidbaur, H. *J. Chem. Soc., Dalton Trans.* **2001**, 1196–1200.

(33) The strain-free values for *gauche* and *anti* conformations are 60° and 180°, respectively.

(34) Ueda, I.; Nowacki, W. Z. *Kristallogr.* **1974**, *139*, 70–84.

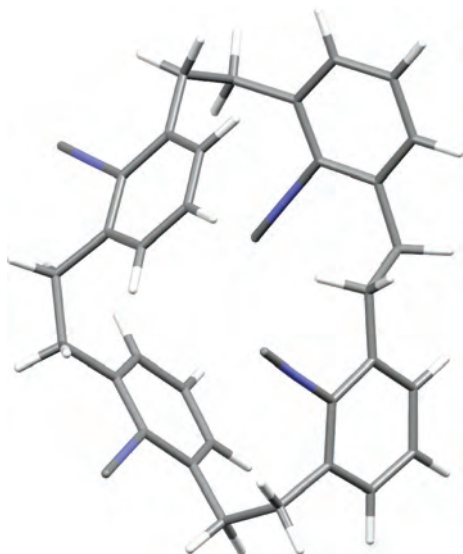


**Figure 4.** DFT-optimized structure of **3** (lowest energy conformation found in this study).

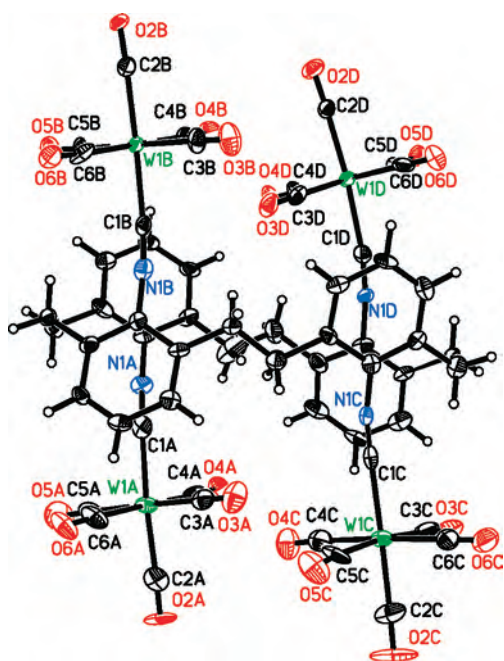


**Figure 5.** Molecular structure of **5** in the solid state (50% thermal ellipsoids). Two disordered  $\text{CH}_2\text{Cl}_2$  molecules of crystallization are omitted.

tetrametallic complex in solution (*vide supra*). The metric parameters of the octahedral  $[(\text{OC})_5\text{W}(\text{CN})]$  moieties within **5** are comparable to the corresponding values recently documented for the  $[\text{W}(\text{CO})_5]$  adducts of 2,6-diisocyanazulene, the only other crystallographically characterized  $(\text{OC})_5\text{W}(\text{CNAr})$  species.<sup>4b</sup> While the C–N–C angles in **3** are essentially linear, minor bending at the nitrogen atoms ( $7\text{--}12^\circ$ ) occurs in **5**. Similar distortions, which have minute energetic consequences,<sup>35</sup> have been observed for the complexes of 2,6-diisocyanazulene with  $[\text{W}(\text{CO})_5]$ .<sup>4b</sup>

**Self-Assembled Monolayers of 3 on Gold.** Properties of SAMs of organic isocyanides on metal surfaces are often

(35) Wagner, N. L.; Kloss, J. M.; Murphy, K. L.; Bennett, D. W. *J. Chem. Inf. Comput. Sci.* **2001**, *41*, 50–55.

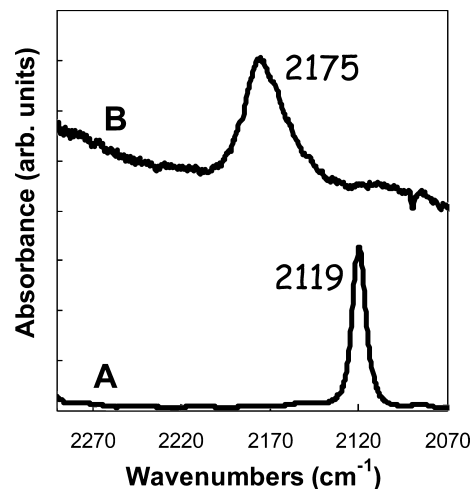


**Figure 6.** FTIR spectra of **3** in  $\text{CH}_2\text{Cl}_2$  solution (A) and adsorbed to the gold(111) surface (B). Spectrum B was obtained using a 2-day-old sample prepared and stored without exclusion of air.

compared or contrasted with those of organic thiols.<sup>5–13</sup> Reinhoudt et al. have demonstrated that [1.1.1]metacyclophane-based organic surfaces on metallic gold can be built by self-assembly of the corresponding cyclophane molecules derivatized with four long-chain alkyl thiol moieties, which serve as anchors.<sup>36</sup> Based on the geometry of the structure shown in Figure 5, one might expect that metacyclophane **3** should be capable of binding to the Au(111) surface via at least two of its isocyanide groups. Angelici,<sup>37</sup> Kubiak,<sup>38</sup> McCarley,<sup>39</sup> and their co-workers have already shown that alkyl di- and triisocyanides with reasonably flexible hydrocarbon substituents adsorb to metallic gold via all of their  $-\text{NC}$  junctions, at least at low coverage. Notably, aryl isocyanide films on metallic gold usually require handling in inert atmosphere to prevent their rapid deterioration. Degradation of the aryl isocyanide-based SAMs involves gold-facilitated oxidation of the metal-bound isocyanide functionality to form the isocyanate group,  $-\text{NCO}$  ( $\nu \approx 2270 \text{ cm}^{-1}$ ), as has been recently demonstrated in a thorough study by Allara et al.<sup>10</sup> The SAMs of 2,6-dimethyl-substituted isocyanoarenes are not immune to oxidative degradation either.<sup>11</sup>

Exposure of a freshly cleaned Au(111) surface to a solution of **3** in dichloromethane *under ambient conditions* resulted in the formation of an air-stable film, FTIR and ellipsometric thickness characteristics (*vide infra*) of which remained unchanged for days. As illustrated in Figure 6, the frequency of the isocyanide stretching vibration increases from  $2119 \text{ cm}^{-1}$  in  $\text{CH}_2\text{Cl}_2$  to  $2175 \text{ cm}^{-1}$  upon adsorption of **3** to the gold surface. This  $56 \text{ cm}^{-1}$  change in  $\nu_{\text{CN}}$  is consistent with terminal upright coordination of the isocyanide groups and

(36) For example: (a) Schierbaum, K.-D.; Weiss, T.; Thoden van Velzen, E. U.; Engbersen, J. F. J.; Reinhoudt, D. N.; Göpel, W. *Science* **1994**, *265*, 1413–1415. (b) Thoden van Velzen, E. U.; Engbersen, J. F. J.; Reinhoudt, D. N. *J. Am. Chem. Soc.* **1994**, *116*, 3597–3598. (c) Huisman, B.-H.; Thoden van Velzen, E. U.; van Veggel, F. C. J. M.; Engbersen, J. F. J.; Reinhoudt, D. N. *Tetrahedron Lett.* **1995**, *36*, 3273–3276.

(37) Ontko, A. C.; Angelici, R. J. *Langmuir* **1998**, *14*, 3071–3078.

(38) Henderson, J. I.; Feng, S.; Bein, T.; Kubiak, C. P. *Langmuir* **2000**, *16*, 6183–6187.

(39) Lin, S.; McCarley, R. L. *Langmuir* **1999**, *15*, 151–159.



**Table 3.** Relative Energies of Ten Hypothetical Conformations of **3** Coordinated to Au(111) in the  $\eta^1:\eta^1:\eta^1:\eta^1$  Fashion<sup>a</sup>

structure	$d_x$ (Å)	$d_y$ (Å)	$\alpha$ (deg)	$\beta$ (deg)	$\Delta E$ (kcal/mol)
a	8.65	8.65	60	120	125.9
b	7.63	7.63	60	120	92.4
c	5.76	5.76	60	120	14.3
d	4.99	4.99	60	120	0.0
e	8.65	4.99	90	90	31.4
f	8.65	5.76	60	120	81.2
g	8.65	7.63	79.1	100.9	33.4
h	5.76	7.63	79.1	100.9	29.2
i	7.63	4.99	70.9	109.1	24.1
j	5.76	4.99	90	90	1.8

<sup>a</sup> The terminal  $-\text{NC}$  carbon atom positions were restricted to match various combinations of Au(111) interatomic distances ( $d_x$ ,  $d_y$ ) and angles ( $\alpha$ ,  $\beta$ ) illustrated in Figure 7.

compares well with that observed for the adsorption of CNXyl, a monomeric analogue of **3** ( $2117\text{ cm}^{-1}$  in  $\text{CH}_2\text{Cl}_2$  vs  $2170\text{ cm}^{-1}$  on Au surface<sup>40</sup>), and to those reported for the chemisorptions of other aryl isocyanides on gold.<sup>4a,5,6,8–13,38</sup>

The FTIR spectrum of **3** adsorbed on Au(111) lacks any features attributable to free isocyanide groups and, therefore, indicates interaction of the molecule with the gold surface via all four of its isocyanide anchors. The width of the relatively symmetric  $\nu_{\text{CN}}$  band in Figure 6B (fwhm  $\approx 25\text{ cm}^{-1}$ ) is comparable to those of the  $\nu_{\text{CN}}$  peaks observed for SAMs of isocyanoarenes  $\eta^1$ -bound to metallic gold in the terminal fashion.<sup>4a,10–12</sup> Imperfections in topology of the Au(111) films prepared by physical vapor deposition are known to contribute to the broadness of these  $\nu_{\text{CN}}$  bands for SAMs of isocyanoarenes on Au(111).<sup>41</sup> The blue shift in  $\nu_{\text{CN}}$  upon coordination of **3** to Au is associated with somewhat antibonding character (with respect to the  $\text{C}\equiv\text{N}$  bond) of the isocyanide carbon's lone pair used in the Au–C bond formation.<sup>42</sup> Importantly, the spectrum shown in Figure 6B is void of a detectable band at ca.  $2270\text{ cm}^{-1}$ , which would have indicated at least partial oxidation of the SAM.

For **3** chemisorbed on gold, the film thickness was probed by ellipsometry in different spots on the sample. The average measured thickness of  $5.8(5)^{43}\text{ \AA}$  confirmed the monolayer nature of the film. This value compares reasonably with the length of the aryl isocyanide moieties in **3** ( $6.4\text{ \AA}$ ) determined from the terminal isocyanide carbon to the hydrogen atom in *para*-position with respect to the  $-\text{NC}$  group. Thus, both FTIR and ellipsometric thickness characteristics of **3** on gold are consistent with the upright coordination of the aryl isocyanide moieties of **3**, roughly perpendicular to the metal surface. We note that the above comparison between the experimental and expected monolayer thicknesses must be taken with caution as it does not consider the possibility of optical contribution from the Au–C interface, the true magnitude of which is not trivial to determine with good accuracy.<sup>10,44</sup>

**DFT Calculations.** In order to estimate the energy cost associated with accessing the conformations of **3** that are

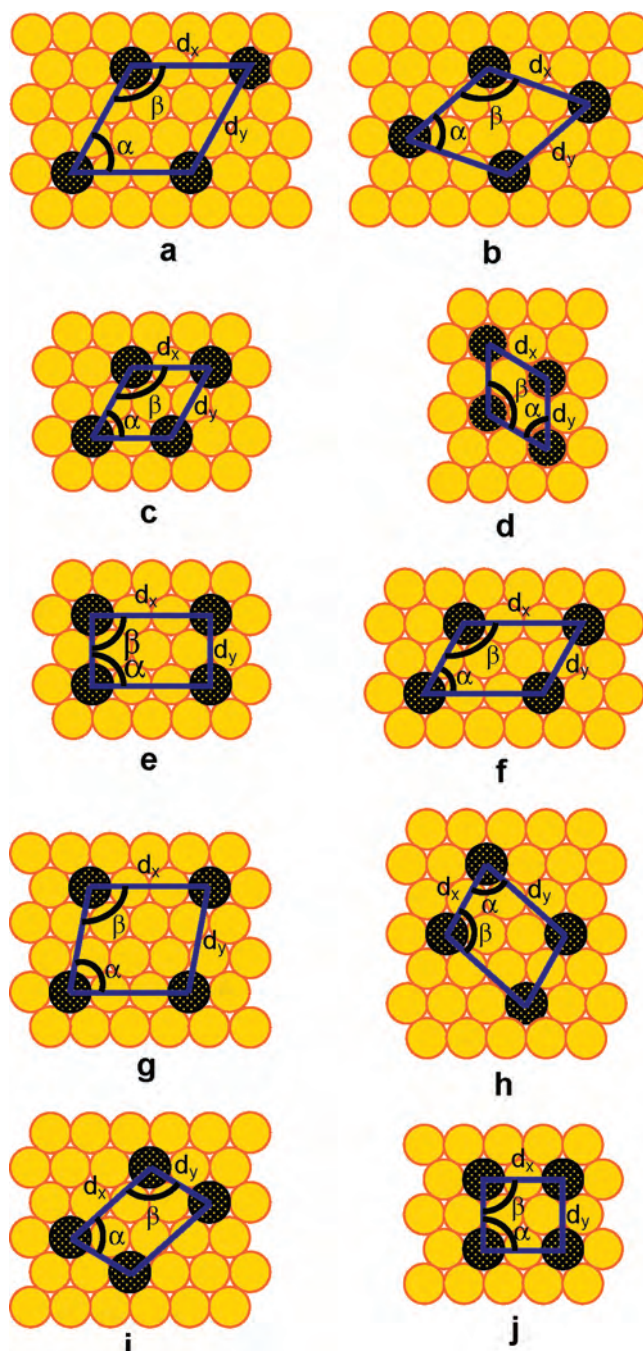


**Figure 7.** Ten combinations of interatomic distances ( $d_x$ ,  $d_y$ ) and angles ( $\alpha$ ,  $\beta$ ) between the gold atoms on the Au(111) surface considered for  $\eta^1:\eta^1:\eta^1:\eta^1$  interaction with tetraisocyanide **3**.

suitable for interaction of the molecule with the gold surface in the upright fashion via all four of its isocyanide anchors, ten different scenarios were screened by DFT at the 3-21G\* level. In these, the initial geometries of **3** were chosen to have four terminal isocyanide carbon atoms restrained to lie in a plane that would be parallel to the gold surface upon coordination of the tetraisocyanide. In addition, the interatomic distances and angles between these carbon atoms were fixed to match one of ten combinations of the interatomic distances and angles involving four gold atoms on the (111) surface of the fcc Au lattice (Table 3 and Figure 7).

Optimization of the above restrained structures yielded two conformations of **3** within 1.8 kcal/mol from each other

(40) Kim, N. H.; Kim, K. *J. Phys. Chem. B* **2006**, *110*, 1837–1842.

(41) Lazar, M.; Angelici, R. J. *J. Am. Chem. Soc.* **2006**, *128*, 10613–10620.

(42) Treichel, P. M. *Adv. Organomet. Chem.* **1973**, *11*, 21–86.

(43) Note that the typical error of such ellipsometric measurements is  $\pm 1\text{ \AA}$ .

(44) Shi, J.; Hong, B.; Parikh, A. N.; Collins, R. W.; Allara, D. L. *Chem. Phys. Lett.* **1995**, *246*, 90–94.

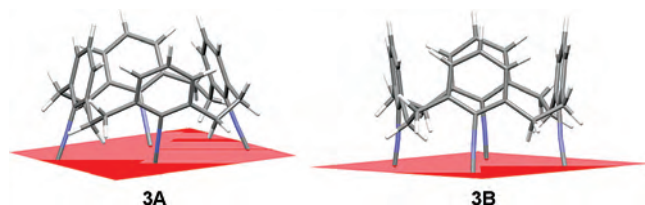


**Figure 8.** Two lowest energy conformations of **3** appropriate for binding to Au(111) in the upright fashion. The positions of the terminal isocyanide carbon atoms were restricted to lie in the same plane and match interatomic distances and angles involving a combination of four Au atoms on the Au(111) surface. For gold atoms on the Au(111) surface involved in coordination with **3**, refer to case d for conformation **3A** and case j for conformation **3B** in Table 3 and Figure 7.

(structures d and j in Table 3) that were clearly energetically preferred over the remaining eight geometries (by at least 12 kcal/mol). These two cases were then considered further using the 6-31+G\* basis set. At this higher level, the two lowest energy conformations of **3** constrained as described above and shown in Figure 8 proved essentially isoenergetic, with structure **B** being only 0.2 kcal/mol destabilized with respect to **A**. The C–N–C units within both **A** (177.1°, 179.4°) and **B** (173.3°, 173.7°) are nearly linear, which is consistent with the experimental FTIR data for **3** adsorbed on gold. It is important to note that the optimized constrained conformations of **3** shown in Figure 8 are less than 8 kcal/mol destabilized compared with the structure of “free” **3** shown in Figure 4. This energy cost can be easily offset by the formation of even one gold–isocyanide bond (ca. 20 kcal/mol).<sup>45</sup> Thus, the adsorption of **3** to gold(111) via all four of its –NC anchors is clearly favorable energetically. In which mode, **A** or **B**, tetraisocyanide **3** would coordinate to the surface is less clear. Structure **3A** would result in somewhat greater tilting of the isocyanoarene units with respect to the gold surface (14° and 16°) than **3B** (5° and 1°). This suggests that **3B** may represent a better candidate for the formation of monolayers through more efficient packing. However, the overall molecular tilting could be significantly influenced by intermolecular interactions within the SAM,<sup>10,38</sup> and additional theoretical and experimental work is needed to confirm this speculation.

(45) (a) Kim, S.; Ihm, K.; Kang, T.-H.; Hwang, S.; Joo, S.-W. *Surf. Interface Anal.* **2005**, *37*, 294–299. (b) Zhou, J.-H.; Shi, L.-W.; Zhang, T.; Chen, M.-B. *Chin. J. Chem.* **2007**, *25*, 1223–1228.

## Concluding Remarks

The structure of tetraisocyano[2.2.2.2]metacyclophane **3**, which can now be synthesized in gram quantities at a time, is mobile in solution but can be locked in the *gauche–anti–gauche–anti* conformation by coordination of the isocyanide substituents to four [W(CO)<sub>5</sub>] fragments. The [M]<sub>4</sub>(μ<sub>4</sub>-η<sup>1</sup>:η<sup>1</sup>:η<sup>1</sup>:η<sup>1</sup>-**3**) motif featured in crystallographically characterized complex **5** constitutes a new building block for 3D coordination architectures. Such μ<sub>4</sub>-η<sup>1</sup>:η<sup>1</sup>:η<sup>1</sup>:η<sup>1</sup> coordination may also be present in the insoluble complexes of **3** previously described as mononuclear η<sup>4</sup> species.<sup>21</sup> Metacyclophane **3** adsorbs on the gold(111) surface via all four of its isocyanide groups and features approximately upright orientation of the aryl isocyanide moieties with respect to the surface, which makes the description of the adsorbed metacyclophane in terms of its inner and outer rims<sup>20,22</sup> meaningful. Remarkably, unlike many benzenoid isocyanoarene SAMs on gold, the SAMs of **3** on Au(111) can be prepared and handled in ambient atmosphere. Two different μ<sub>4</sub>-η<sup>1</sup>:η<sup>1</sup>:η<sup>1</sup>:η<sup>1</sup> coordination arrangements of **3** adsorbed on Au(111) have been suggested by DFT. The energetic gain upon chemisorption of **3** to the gold surface in the μ<sub>4</sub>-η<sup>1</sup>:η<sup>1</sup>:η<sup>1</sup>:η<sup>1</sup> fashion substantially outweighs the cost of the metacyclophane conformational change required for such coordination. Thus, isocyanide groups can function as effective two-atom long anchors for self-assembling stable monolayers of cyclophanes on metallic gold, and the strategy described herein should be of general utility. Imaging studies of the SAMs of **3** and its derivatives chemisorbed on Au(111), as well as synthesis of other tetraisocyanofunctionalized cyclophanes and adsorption thereof on metallic gold, are in progress.

**Acknowledgment.** This work was largely supported by the National Science Foundation (NSF CAREER Award CHE-0548212 to M.V.B.). The authors thank Dr. Douglas R. Powell for his expert assistance in the crystallographic characterization of **3**.

**Supporting Information Available:** Spectroscopic characterization data for **3**, **4**, and **5**, complete crystallographic information for **3** and **5**·2CH<sub>2</sub>Cl<sub>2</sub> in CIF format, Cartesian coordinates files pertaining to DFT calculations, and complete ref 27. This material is available free of charge via the Internet at <http://pubs.acs.org>.

IC702401B